ISSN 1674-1056
http://cpb.iphy.ac.cn
http://iopscience.iop.org/cpb
中国物理 B
Chinese Physics
中国物理
Chinese Physics B

Dynamics of traveling wave solutions to a highly nonlinear Fujimoto-Watanabe equation

Li-Juan Shi(师利娟), Zhen-Shu Wen(温振庶)

Citation: Chin. Phys. B . 2019, 28(4): 040201. **doi:** 10.1088/1674-1056/28/4/040201
Journal homepage: http://cpb.iphy.ac.cn; http://iopscience.iop.org/cpb

What follows is a list of articles you may be interested in

Evolutionary game dynamics of combining the Moran and imitation processes

Xian-Jia Wang(王先甲), Cui-Ling Gu(顾翠伶), Shao-Jie Lv(吕少杰), Ji Quan(全吉)
Chin. Phys. B . 2019, 28(2): 020203. **doi:** 10.1088/1674-1056/28/2/020203

Growth mode of helium crystal near dislocations in titanium

Bao-Ling Zhang(张宝玲), Bao-Wen Wang(王保文), Xue Su(苏雪), Xiao-Yong Song(宋小勇), Min Li(李敏)
Chin. Phys. B . 2018, 27(6): 060205. **doi:** 10.1088/1674-1056/27/6/060205

Temperature dependence of migration features of self-interstitials in zirconium

Rui Zhong(钟睿), Qing Hou(侯氢), Chao-Qiong Ma(马超琼), Bao-Qin Fu(付宝勤), Jun Wang(汪俊)
Chin. Phys. B . 2017, 26(12): 120202. **doi:** 10.1088/1674-1056/26/12/120202

An intermediate state of T7 RNA polymerase provides another pathway of nucleotide selection

Zhan-Feng Wang(王展峰), Yu-Ru Liu(刘玉如), Peng-Ye Wang(王鹏业), Ping Xie(谢平)
Chin. Phys. B . 2017, 26(10): 100203. **doi:** 10.1088/1674-1056/26/10/100203

Geometry and thermodynamics of smeared Reissner-Nordström black holes in *d*-dimensional AdS spacetime

Bo-Bing Ye(叶伯兵), Ju-Hua Chen(陈菊华), Yong-Jiu Wang(王永久)
Chin. Phys. B . 2017, 26(9): 090202. **doi:** 10.1088/1674-1056/26/9/090202

Dynamics of traveling wave solutions to a highly nonlinear Fujimoto–Watanabe equation*

Li-Juan Shi(师利娟) and Zhen-Shu Wen(温振庶)†

Fujian Province University Key Laboratory of Computational Science, School of Mathematical Sciences, Huaqiao University, Quanzhou 362021, *China*

(Received 27 December 2018; revised manuscript received 31 January 2019; published online 19 March 2019)

In this work, we apply the bifurcation method of dynamical systems to investigate the underlying complex dynamics of traveling wave solutions to a highly nonlinear Fujimoto–Watanabe equation. We identify all bifurcation conditions and phase portraits of the system in different regions of the three-dimensional parametric space, from which we present the sufficient conditions to guarantee the existence of traveling wave solutions including solitary wave solutions, periodic wave solutions, kink-like (antikink-like) wave solutions, and compactons. Furthermore, we obtain their exact expressions and simulations, which can help us understand the underlying physical behaviors of traveling wave solutions to the equation.

Keywords: highly nonlinear Fujimoto–Watanabe equation, dynamics, traveling wave solutions, bifurcations

PACS: 02.30.Hq, 02.30.Oz, 05.45.Yv, 05.45.–a **DOI:** 10.1088/1674-1056/28/4/040201

1. Introduction

Eight third-order differential equations and two fifth-order differential equations are derived by Fujimoto and Watanabe,[1] and among these equations, one highly nonlinear Fujimoto–Watanabe equation possesses the following form

$$u_t = u^3 u_{xxx} + \alpha u^3 u_x, \tag{1}$$

where α is a parameter, when they classified the third-order polynomial evolution equations of uniform rank with non-constant separants, which admit generalized symmetries (non-trivial Lie–Bäcklund algebras). Fujimoto and Watanabe[1] have shown that equation (1) possesses the hereditary recursion operator of Lie–Bäcklund symmetries, which means that the Lie algebras of its Lie–Bäcklund symmetries are infinite-dimensional and commutative. However, they did not prove its integrability.[2] Sakovich[3] further showed that these differential equations can be connected with the famous KdV equation, Qiao equation,[4] and so on, via chains of differential substitutions. Note that there have little studies about Eq. (1), because of its high nonlinearity (precisely, quartic nonlinearity), in our opinion. Here we find a way to handle its high nonlinearity, according to its specific structures. Shi and Wen[5,6] studied traveling wave solutions to two of these Fujimoto–Watanabe equations and showed that these traveling wave solutions possess abundant dynamical behaviors. One may consider what about the dynamics of traveling wave solutions to other Fujimoto–Watanabe equations. Driven by this motivation, in this work, we aim at dynamics of traveling wave solutions to Eq. (1) from the the perspective of the theory of dynamical systems.[7–14]

More precisely, we first transform Eq. (1) into a planar system by substituting $u(x,t) = \varphi(\xi)$ with $\xi = x - ct$ into Eq. (1), which yields

$$-c\varphi' = \varphi^3\varphi''' + \alpha\varphi^3\varphi', \tag{2}$$

where the prime stands for the derivative with respect to ξ.

Dividing both sides of Eq. (2) by φ^2 and then integrating it once, we obtain

$$\frac{c}{\varphi} + g = \varphi\varphi'' + \frac{\alpha\varphi^2}{2} - \frac{\varphi'^2}{2}, \tag{3}$$

where g is the integral constant.

Letting $y = \varphi'$, we obtain a three-parameter planar system

$$\begin{cases} \dfrac{\mathrm{d}\varphi}{\mathrm{d}\xi} = y, \\ \dfrac{\mathrm{d}y}{\mathrm{d}\xi} = \dfrac{-\alpha\varphi^3 + 2c + \varphi y^2 + 2g\varphi}{2\varphi^2}, \end{cases} \tag{4}$$

with first integral

$$H(\varphi, y) = \frac{y^2}{2\varphi} + \frac{\alpha\varphi}{2} + \frac{g}{\varphi} + \frac{c}{2\varphi^2}. \tag{5}$$

Note that if $c = 0$, system (4) becomes a different system

$$\begin{cases} \dfrac{\mathrm{d}\varphi}{\mathrm{d}\xi} = y, \\ \dfrac{\mathrm{d}y}{\mathrm{d}\xi} = \dfrac{-\alpha\varphi^2 + y^2 + 2g}{2\varphi}, \end{cases} \tag{6}$$

the phase portraits of which should be analyzed individually.

Of particular interest of this paper is to study complex dynamics of traveling wave solutions to system (4) in the three-dimensional parameter space (α, c, g) and to show their exact expressions and simulations, which can fascinate the underlying physical behaviors of traveling wave solutions to Eq. (1).

*Project supported by the National Natural Science Foundation of China (Grant Nos. 11701191 and 11871232), the Program for Innovative Research Team in Science and Technology in University of Fujian Province, Quanzhou High-Level Talents Support Plan (Grant No. 2017ZT012), and the Subsidized Project for Cultivating Postgraduates' Innovative Ability in Scientific Research of Huaqiao University.

†Corresponding author. E-mail: wenzhenshu@hqu.edu.cn

© 2019 Chinese Physical Society and IOP Publishing Ltd

2. Bifurcation conditions and phase portraits

Note that system (4) is not well-defined on the line $l: \varphi = 0$. Therefore, we consider the associated system of system (4) as follows:

$$\begin{cases} \dfrac{\mathrm{d}\varphi}{\mathrm{d}\tau} = \varphi^2 y, \\ \dfrac{\mathrm{d}y}{\mathrm{d}\tau} = -\dfrac{\alpha\varphi^3}{2} + \frac{\varphi y^2}{2} + g\varphi + c, \end{cases} \tag{7}$$

where $\mathrm{d}\xi = \varphi^2 \mathrm{d}\tau$.

We can analyze the phase portraits of system (4) from those of system (7), since system (7) has the same level curves as system (4).

To study the singular points and their properties of system (7), let

$$f(\varphi) = -\frac{\alpha\varphi^3}{2} + g\varphi + c. \tag{8}$$

We can easily obtain the graphics of the function $f(\varphi)$ in Figs. 1 and 2 in corresponding parametric space.

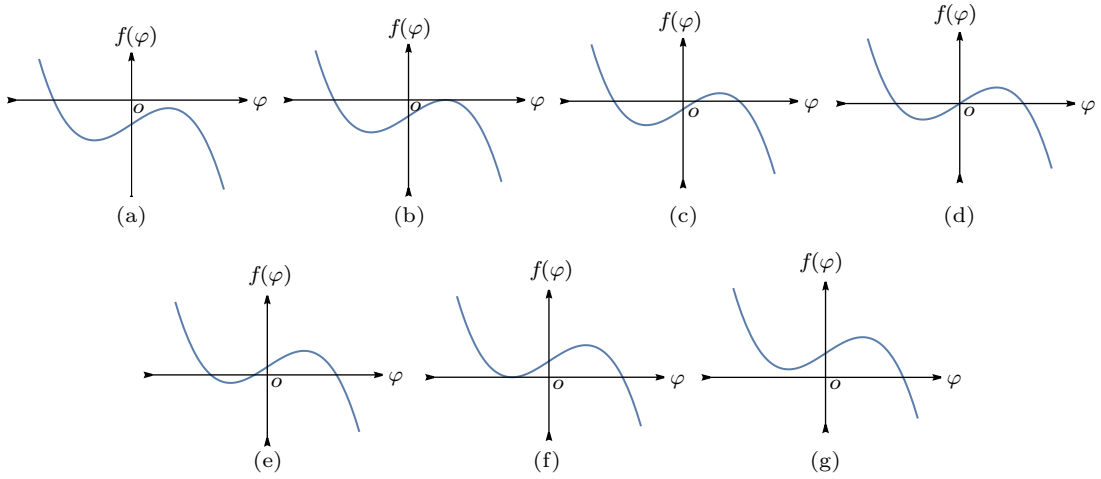


Fig. 1. The graphics of $f(\varphi)$ when $\alpha > 0$ and $g > 0$. (a) $c < -(2g/3)\sqrt{2g/3\alpha}$, (b) $c = -(2g/3)\sqrt{2g/3\alpha}$, (c) $-(2g/3)\sqrt{2g/3\alpha} < c < 0$, (d) $c = 0$, (e) $0 < c < (2g/3)\sqrt{2g/3\alpha}$, (f) $c = (2g/3)\sqrt{2g/3\alpha}$, and (g) $c > (2g/3)\sqrt{2g/3\alpha}$.

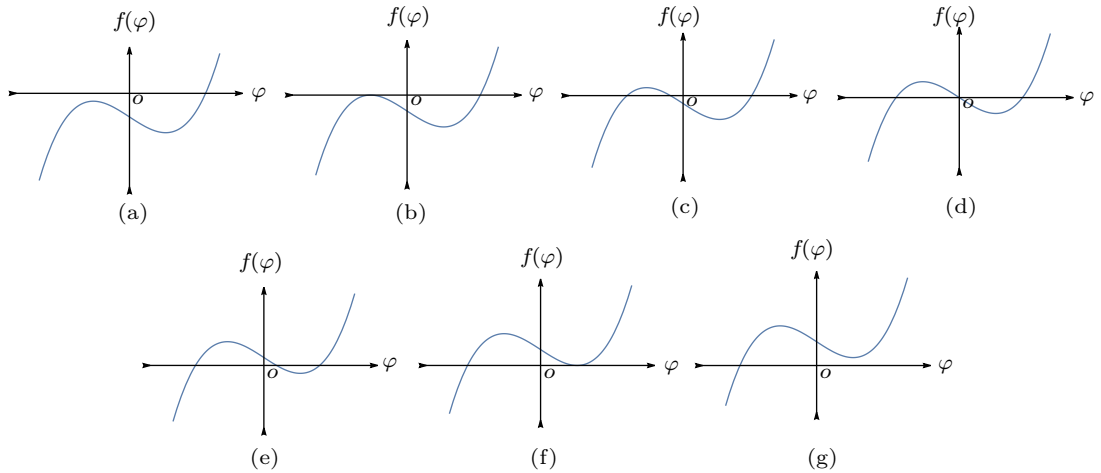


Fig. 2. The graphics of $f(\varphi)$ when $\alpha < 0$ and $g < 0$. (a) $c < (2g/3)\sqrt{2g/3\alpha}$, (b) $c = (2g/3)\sqrt{2g/3\alpha}$, (c) $(2g/3)\sqrt{2g/3\alpha} < c < 0$, (d) $c = 0$, (e) $0 < c < -(2g/3)\sqrt{2g/3\alpha}$, (f) $c = -(2g/3)\sqrt{2g/3\alpha}$, and (g) $c > -(2g/3)\sqrt{2g/3\alpha}$.

Let $\lambda(\varphi, y)$ be the characteristic value of the linearized system of system (7) at the singular point (φ, y). We easily obtain

$$\lambda^2(\varphi_i, 0) = (\varphi_i)^2 f'(\varphi_i). \tag{9}$$

From Eq. (9), we see that the sign of $f'(\varphi_i)$ can determine the dynamical properties (saddle, center, and degenerate singular point) of the singular point $(\varphi_i, 0)$ according to the theory of planar dynamical systems.

Now we summarize the singular points of system (7) and their relative positions when $\alpha > 0$, $g > 0$ in the following lemma. We just omit the other case when $\alpha < 0$, $g < 0$, since it can be analyzed similarly.

Lemma 1 When $\alpha > 0$, $g > 0$, the singular points of system (7) are as follows.

(i) When $c < -(2g/3)\sqrt{2g/3\alpha}$, system (7) has only one singular point $(\varphi_1, 0)$ with $\varphi_1 < 0$.

(ii) When $c = -(2g/3)\sqrt{2g/3\alpha}$, system (7) has two singular points $(\varphi_1, 0)$ and $(\varphi_2, 0)$ with $\varphi_1 < 0 < \varphi_2 = \varphi_3$.

(iii) When $-(2g/3)\sqrt{2g/3\alpha} < c < 0$, system (7) has

three singular points $(\varphi_1,0)$, $(\varphi_2,0)$ and $(\varphi_3,0)$ with $\varphi_1<0<\varphi_2<\varphi_3$.

(iv) When $c=0$, system (7) has three singular points $(\varphi_1,0)$, $(\varphi_2,0)$ and $(\varphi_3,0)$ with $\varphi_1<\varphi_2=0<\varphi_3$.

(v) When $0<c<(2g/3)\sqrt{2g/3\alpha}$, system (7) has three singular points $(\varphi_1,0)$, $(\varphi_2,0)$ and $(\varphi_3,0)$ with $\varphi_1<\varphi_2<0<\varphi_3$.

(vi) When $c=(2g/3)\sqrt{2g/3\alpha}$, system (7) has two singular points $(\varphi_1,0)$ and $(\varphi_3,0)$ with $\varphi_1=\varphi_2<0<\varphi_3$.

(vii) When $c>(2g/3)\sqrt{2g/3\alpha}$, system (7) has only one singular point $(\varphi_3,0)$ with $\varphi_3>0$.

Through qualitative analysis, we obtain all possible bifurcations of phase portraits of system (4) in Figs. 3 and 4, respectively.

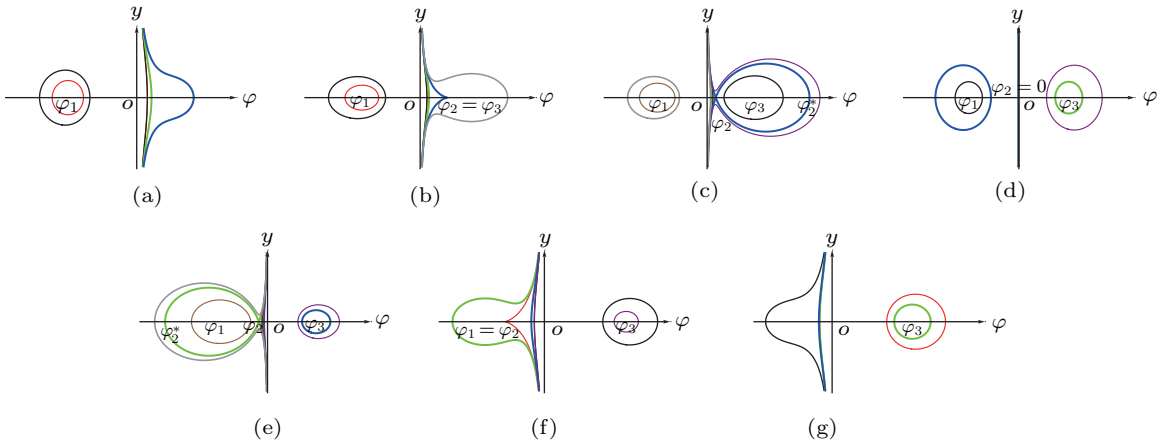


Fig. 3. The phase portraits of system (5) when $\alpha>0$ and $g>0$. (a) $c<-(2g/3)\sqrt{2g/3\alpha}$, (b) $c=-(2g/3)\sqrt{2g/3\alpha}$, (c) $-(2g/3)\sqrt{2g/3\alpha}<c<0$, (d) $c=0$, (e) $0<c<(2g/3)\sqrt{2g/3\alpha}$, (f) $c=(2g/3)\sqrt{2g/3\alpha}$, and (g) $c>(2g/3)\sqrt{2g/3\alpha}$.

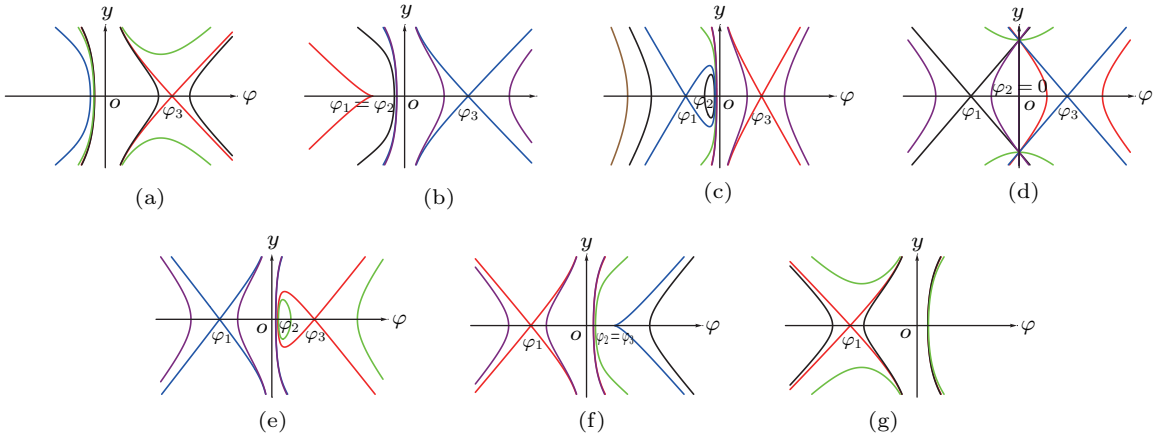


Fig. 4. The phase portraits of system (5) when $\alpha<0$ and $g<0$. (a) $c<(2g/3)\sqrt{2g/3\alpha}$, (b) $c=(2g/3)\sqrt{2g/3\alpha}$, (c) $(2g/3)\sqrt{2g/3\alpha}<c<0$, (d) $c=0$, (e) $0<c<-(2g/3)\sqrt{2g/3\alpha}$, (f) $c=-(2g/3)\sqrt{2g/3\alpha}$, and (g) $c>-(2g/3)\sqrt{2g/3\alpha}$.

3. Main results and the theoretic derivations of main results

Our main results will be stated in the following theorems, and the proofs follow.

Theorem 1 When $\alpha>0$ and $g>0$, one has

I) When $c\le-(2g/3)\sqrt{2g/3\alpha}$ or $c\ge(2g/3)\sqrt{2g/3\alpha}$, there exist a family of periodic wave solutions to Eq. (1). When $-(2g/3)\sqrt{2g/3\alpha}<c<(2g/3)\sqrt{2g/3\alpha}$, there exist two families of periodic wave solutions to Eq. (1).

II) When $-(2g/3)\sqrt{2g/3\alpha}\le c<0$ or $0<c\le(2g/3)\sqrt{2g/3\alpha}$, there exist a pair of kink-like (antikink-like) wave solutions to Eq. (1). Specially, taking $c=-(2g/3)\sqrt{2g/3\alpha}$, the pair of kink-like (antikink-like) wave solutions possess the expression

$$\sqrt{\frac{\varphi}{\varphi_2-\varphi}}-\sqrt{\frac{\varphi_0}{\varphi_2-\varphi_0}}-\arctan\sqrt{\frac{\varphi}{\varphi_2-\varphi}}+\arctan\sqrt{\frac{\varphi_0}{\varphi_2-\varphi_0}}=\frac{\sqrt{\alpha}}{2}|x-ct|, \tag{10}$$

where $\varphi_2=\sqrt{2g/3\alpha}$.

III) When $-(2g/3)\sqrt{2g/3\alpha}<c<0$ or $0<c<(2g/3)\sqrt{2g/3\alpha}$, there exists a solitary wave solution to Eq. (1). Specifically, when $-(2g/3)\sqrt{2g/3\alpha}<c<0$, the solitary wave solution possesses the expression

$$-\sqrt{\frac{\varphi_2}{\varphi_2^*-\varphi_2}}\ln\left(\frac{\sqrt{\varphi/(\varphi_2^*-\varphi)}-\sqrt{\varphi_2/(\varphi_2^*-\varphi_2)}}{\sqrt{\varphi/(\varphi_2^*-\varphi)}+\sqrt{\varphi_2/(\varphi_2^*-\varphi_2)}}\right)$$

$$+2\left(\frac{\pi}{2}-\arctan\sqrt{\frac{\varphi}{\varphi_2^*-\varphi}}\right)=\sqrt{\alpha}|x-ct|, \tag{11}$$

where $\varphi_2=\lambda\sqrt{2g/3\alpha}$ and $\varphi_2^*=-c/(\alpha(\varphi_2)^2)$ with $0<\lambda<1$.

IV) When $c<-(2g/3)\sqrt{2g/3\alpha}$ or $c>(2g/3)\sqrt{2g/3\alpha}$, there exist a family of compactons to Eq. (1). When $-(2g/3)\sqrt{2g/3\alpha}\le c<0$ or $0<c\le(2g/3)\sqrt{2g/3\alpha}$, there exist two families of compactons to Eq. (1).

Proof

(I) The statements follow from the fact that periodic orbit gives rise to periodic wave solution.

(II) The stable and unstable manifolds, on the left side of singular point $(\varphi_2,0)$ in Figs. 3(b) and 3(c), and on the right side of singular point $(\varphi_2,0)$ in Figs. 3(e) and 3(f), respectively, give rise to kink-like (antikink-like) wave solutions to Eq. (1).[15–19] Here we only illustrate the case when $c=-(2g/3)\sqrt{2g/3\alpha}$.

The stable and unstable manifolds on the left side of singular point $(\varphi_2,0)$ in Fig. 3(b) can be expressed as

$$y=\pm\sqrt{\frac{\alpha(\varphi_2-\varphi)^3}{\varphi}},0<\varphi<\varphi_2. \tag{12}$$

Substituting Eq. (12) into $\mathrm{d}\varphi/\mathrm{d}\xi=y$ and integrating them along the stable and unstable manifolds with $0<\varphi_0<\varphi_2$, it follows that

$$\int_{\varphi_0}^{\varphi}\frac{\sqrt{s}\mathrm{d}s}{(\varphi_2-s)\sqrt{\varphi_2-s}}=\sqrt{\alpha}|\xi|. \tag{13}$$

From Eq. (13), we gain the kink-like (antikink-like) wave solutions as Eq. (10), the graphics of which are shown in Figs. 5(a) and 5(b).

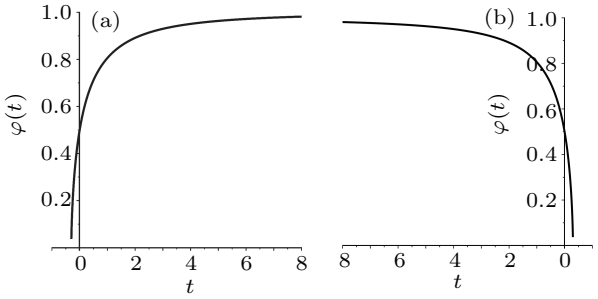


Fig. 5. The graphics of kink-like (antikink-like) wave solutions to Eq. (1): (a) $c=-(2g/3)\sqrt{2g/3\alpha}$ and (b) $c=-(2g/3)\sqrt{2g/3\alpha}$.

(III) When $-(2g/3)\sqrt{2g/3\alpha}<c<0$, from Fig. 3(c), we see that there is one homoclinic orbit for system (4), the expressions of which are given as

$$y=\pm\sqrt{\frac{\alpha(\varphi-\varphi_2)^2(\varphi_2^*-\varphi_2)}{\varphi}},\varphi_2<\varphi<\varphi_2^*. \tag{14}$$

Substituting Eq. (14) into $\mathrm{d}\varphi/\mathrm{d}\xi=y$ and integrating them along the homoclinic orbit, it follows that

$$\int_{\varphi}^{\varphi_2^*}\frac{\sqrt{s}\mathrm{d}s}{(s-\varphi_2)\sqrt{\varphi_2^*-s}}=\sqrt{\alpha}|\xi|. \tag{15}$$

From Eq. (15), we get solitary wave solution Eq. (11).

(IV) We only illustrate the cases when $c<-(2g/3)\sqrt{2g/3\alpha}$ in Fig. 3(a) and $c=-(2g/3)\sqrt{2g/3\alpha}$ in Fig. 3(b), since the other cases can be obtained similarly.

Corresponding to the one family of orbits, passing through the point $(\varphi_0,0)$ with $\varphi_0\in(0,+\infty)$ in Fig. 3(a), equation (1) has a family of compactons as shown in Fig. 6(a).

Corresponding to the two family of orbits, passing through the point $(\varphi_0,0)$ with $\varphi_0\in(0,\varphi_2)\bigcup(\varphi_2,+\infty)$ in Fig. 3(b), equation (1) has two families of compactons as shown in Figs. 6(b) and 6(c).

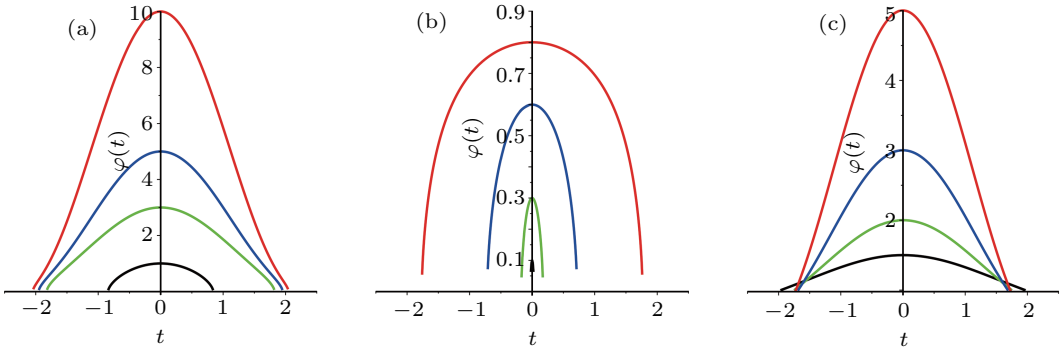


Fig. 6. The graphics of compactons to Eq. (1): (a) $c<-(2g/3)\sqrt{2g/3\alpha}$, (b) $c=-(2g/3)\sqrt{2g/3\alpha}$, and (c) $c=-(2g/3)\sqrt{2g/3\alpha}$.

Similarly, we can get the following results.

Theorem 2 When $\alpha<0$ and $g<0$, one has

I) When $(2g/3)\sqrt{2g/3\alpha}<c<0$ or $0<c<-(2g/3)\sqrt{2g/3\alpha}$, there exist a family of periodic wave solutions and a solitary wave solution to Eq. (1).

II) When $c<0$ or $c>0$, there exist a pair of kink-like (antikink-like) wave solutions and a family of compactons to Eq. (1).

Remark 1 It seems that the form of Eq. (1) is simpler than the equations studies in Refs. [5] and [6]. However, the

traveling wave system Eq. (7) is more complicated than those in Refs. [5] and [6] and possesses more abundant dynamics, such as the the appearance of nodes in the phase portraits.

4. Conclusions

In this paper, through all possible bifurcations for the system in parameter space, we not only show the existence of traveling wave solutions including solitary wave solutions, periodic wave solutions, kink-like (antikink-like) wave solutions, and compactons, under corresponding parameters conditions, but also give their exact expressions and simulations.

References

[1] Fujimoto A and Watanabe Y 1989 *Phys. Lett. A* **136** 294
[2] Shiohama K 1989 *Geometry of Manifolds* (Academic Press)
[3] Sakovich S 1991 *J. Phys. A: Math. Gen.* **24** L519
[4] Sakovich S 2011 *J. Math. Phys.* **52** 023509
[5] Shi L J and Wen Z S 2018 *Commun. Theor. Phys.* **69** 631
[6] Wen Z S and Shi L J 2018 *Chin. Phys. B* **27** 090201
[7] Wen Z S, Liu Z R and Song M 2009 *Appl. Math. Comput.* **215** 2349
[8] Wen Z S and Liu Z R 2011 *Nonlinear Anal. Real.* **12** 1698
[9] Biswas A and Song M 2013 *Commun. Nonlinear Sci.* **18** 1676
[10] Chen A Y, Wen S Q, Tang S Q, Huang W T and Qiao Z J 2015 *Stud. Appl. Math.* **134** 24
[11] Pan C H and Yi Y T 2015 *J. Nonlinear Math. Phys.* **22** 308
[12] Wen Z S 2017 *Nonlinear Dyn.* **87** 1917
[13] Wen Z S 2017 *Int. J. Bifurcat. Chaos* **27** 1750114
[14] Li J B and Qiao Z J 2012 *Int. J. Bifurcat. Chaos* **22** 12500305
[15] Wen Z S 2014 *Nonlinear Dyn.* **77** 849
[16] Wen Z S and Shi L J 2018 *Dyn. Syst. Appl.* **27** 581
[17] Liu Z R and Long Y 2007 *Nonlinear Anal. Real.* **8** 136
[18] Wen Z S 2015 *Nonlinear Dyn.* **82** 767
[19] Li S Y and Liu Z R 2015 *Nonlinear Dyn.* **79** 903